Two kinds of singularities in planar differential systems and the response to external forces

Hu Gang
Physics Department, Beijing Normal University, Beijing 100875, People's Republic of China and Nordisk Institute for Teoretisk Atomfysik, Blegdamsvej 17, 2100 Copenhagen, Denmark

Bai-lin Hao
Institute Theoretical Physics, Academia Sinica, Bejing, Peoples's Republic of China
(Received 20 February 1990)

A Lyapunov function is defined for two-dimensional differential systems. The relationship between the Lyapunov function and the stationary probability distribution of the corresponding Fokker-Planck equations in the weak-noise limit is analyzed. Based on the structure of the Lyapunov function we classify two types of singularities. The classification of different kinds of singularities is shown to be significant for the intrinsical dynamics of the deterministic flow. The bifurcation behavior of periodically forced planar systems that contain distinctive kinds of singularities in the autonomous cases is investigated. It is found that the responses of planar systems to the external force, i.e., the resulting bifurcation sequences, are substantially different if the trajectories circle around different types of singularities.

I. INTRODUCTION

Planar systems of nonlinear differential equations such as

$$\begin{aligned}\dot{x}&=C_1(x,y,t)\ ,\\ \dot{y}&=C_2(x,y,t)\ ,\end{aligned}\tag{1}$$

have been extensively investigated (see Refs. 1 and 2, and references therein) for the following reasons. On one hand, they are capable of producing much richer dynamics in comparison with one-dimensional differential equations. On the other hand, they are still considerably simpler than systems with more than two equations and thus allow for a detailed analysis. Consequently, they have been much better understood than those of higher dimensions. Moreover, planar systems have a wide range of physical applications. Many models of practical relevance, such as the forced pendulum,[3] the Duffing equation,[4–7] and the Van der Pol oscillator,[8] belong to this range.

In this paper we will consider only dissipative planar systems and mainly focus on their attracting sets of solutions. The study of unstable trajectories is also interesting from a mathematical point of view. However, they will not be considered here since they are not directly observable.

Let us first start with an autonomous system

$$\begin{aligned}\dot{x}&=C_1(x,y)\ ,\\ \dot{y}&=C_2(x,y)\ .\end{aligned}\tag{2}$$

One of the most interesting extentions of Eqs. (2) is to include noise and to investigate the response of the system. With the simplest assumption of the noise being Gaussian, Eqs. (2) become Langevin equations:

$$\begin{aligned}\dot{x}&=C_1(x,y)+\gamma_1(t)\ ,\\ \dot{y}&=C_2(x,y)+\gamma_2(t)\ ,\end{aligned}\tag{3}$$

where

$$\langle\gamma_1(t)\rangle=\langle\gamma_2(t)\rangle=\langle\gamma_1(t)\gamma_2(t')\rangle=0\ ,$$
$$\langle\gamma_1(t)\gamma_1(t')\rangle=2\epsilon\delta(t-t')\ ,$$
$$\langle\gamma_2(t)\gamma_2(t')\rangle=2\epsilon\delta(t-t')$$

($\epsilon>0$). System (3) can be transformed into a Fokker-Planck equation (FPE):

$$\begin{aligned}\frac{\partial p(x,y,t)}{\partial t}=&-\frac{\partial}{\partial x}[C_1(x,y)p(x,y,t)]\\ &-\frac{\partial}{\partial y}[C_2(x,y)p(x,y,t)]\\ &+\epsilon\left[\frac{\partial^2}{\partial x^2}+\frac{\partial^2}{\partial y^2}\right]p(x,y,t)\ .\end{aligned}\tag{4}$$

A great number of publications have been devoted to the investigation of this FPE (see, e.g., Refs. 9–19).

Another major approach focuses on the response of system (2) to a regular external source, say, a periodic force:

$$\begin{aligned}\dot{x}&=C_1(x,y)\ ,\\ \dot{y}&=C_2(x,y)+E\cos(\omega t)\ .\end{aligned}\tag{5}$$

It has been known that complicated bifurcation sequences leading to erratic motions may appear, whereas the force remains periodic and well behaved.

Up to date, most of the investigations on (4) and (5)

have been conducted as two distinct fields, apart from a few publications studying the influence of noise on bifurcations at the onset of chaos and some works considering the problem of stochastic resonance.[20–24] In Refs. 15 and 16, one of us has analyzed the potential of FPE (4) in the weak-noise limit ($\epsilon \ll 1$). It has been found that two different types of singularities in Eqs. (2), in particular, two types of saddles, may be distinguished according to the different potential structure of the FPE (see, e.g., the last part of Sec. IV in Ref. 16). It has been well known that in the weak-noise limit the potential of the FPE has a close relation with the corresponding deterministic system. Thus it would be interesting to ask whether these two kinds of singularities, classified on the basis of potential of the FPE, affects the deterministic dynamics or not. The answer to the problem in the present paper is rather positive. Therefore, distinct structures of the potential and, consequently, the classification of singularities may appear to be physically and mathematically meaningful new concepts for planar systems.

In Sec. II, we briefly analyze the potential of the FPE (4) and distinguish two kinds of singularities, in particular, two kinds of saddles, according to the potential. A potential, slightly different from that of the FPE, is suggested. In Sec. III, the dynamics of the deterministic system (2) around these two kinds of singular points will be distinguished. In Sec. IV, we analyze numerically the response of the system to a periodic external force. We shall see that the responses differ considerably if the planar systems contain different kinds of singularities in the autonomous case. In Sec. V, some examples of practical significance, which are supposed to contain different kinds of singularities, are investigated. Section VI summarizes the conditions and distinctions of bifurcations in various periodically forced planar differential systems. In Sec. VII, the discussion of the potential will be extended to FPE with an arbitrary diffusion matrix. The potential obtained for the general FPE confirms the classification of two kinds of singularities. In Sec. VIII, we juxtapose some open problems deserving further investigation.

II. POTENTIAL AND TWO CLASSES OF SINGULAR POINTS

In recent decades, one of the most attracting problems in statistical physics has been to extend the general formalism of equilibrium potential to non equilibrium systems. To this end, the FPE (4) has been extensively used.[9–19] The stationary probability distribution of (4) can be expanded in terms of ϵ as

$$p(x,y)=N\exp\left[-\frac{\phi_0(x,y)}{\epsilon}-\phi_1(x,y)-\epsilon\phi_2(x,y)-\cdots\right] . \tag{6}$$

In the weak-noise limit $\epsilon \ll 1$, only the first term in the large parentheses, i.e., $\phi_0(x,y)/\epsilon$, dominates, and ϕ_0 is often called the potential of the FPE. Inserting (6) into Eq. (4) and keeping only the leading terms of order $1/\epsilon$, we arrive at the Hamilton-Jacobi equation[14,15]

$$C_1(x,y)\frac{\partial\phi_0}{\partial x}+C_2(x,y)\frac{\partial\phi_0}{\partial y}+\left[\frac{\partial\phi_0}{\partial x}\right]^2+\left[\frac{\partial\phi_0}{\partial y}\right]^2=0 . \tag{7}$$

Suppose that we are able to decompose the drift (C_1,C_2) into the following form:

$$\begin{aligned} C_1(x,y)&=g_1(x,y)+d_1(x,y) ,\\ C_2(x,y)&=g_2(x,y)+d_2(x,y) , \end{aligned} \tag{8}$$

under the conditions

$$\begin{aligned} &\frac{\partial g_1}{\partial y}=\frac{\partial g_2}{\partial x}=-\frac{\partial^2\psi_0}{\partial x\,\partial y} ,\\ &g_1d_1+g_2d_2=0 . \end{aligned} \tag{9}$$

It is evident that the function $\psi_0(x,y)$ must be a solution of (7) and, at the same time, be a Lyapunov function of the deterministic system (2):

$$\dot{\psi}_0=-(g_1^2+g_2^2)\le 0 , \tag{10}$$

which must reach extrema on all the asymptotic sets of (2). Let us consider a limit cycle system. Then ψ_0 should take extrema along the entire limit cycle, i.e., the constraints

$$g_1=\frac{\partial\psi_0}{\partial x}=g_2=\frac{\partial\psi_0}{\partial y}=0 \tag{11}$$

should hold on a one-dimensional closed curve. Thus it is convenient to rewrite (g_1,g_2) as (Qa_1,Qa_2) with $Q=0$ yielding the limit cycle.[16] Therefore, Eqs. (8) can be replaced by

$$\begin{aligned} C_1(x,y)&=\mu Q(x,y)a_1(x,y)-\zeta f(x,y)a_2(x,y) ,\\ C_2(x,y)&=\mu Q(x,y)a_2(x,y)+\zeta f(x,y)a_1(x,y) , \end{aligned} \tag{12}$$

with

$$\frac{\partial(Qa_1)}{\partial y}=\frac{\partial(Qa_2)}{\partial x}=-\frac{\partial^2\psi_0}{\partial x\,\partial y} . \tag{13}$$

Note, however, that the choice of $Q(x,y)$, which vanishes on the limit cycle, is associated with some uncertainty. Nevertheless, this uncertainty does not affect the potential. Moreover, (a_1,a_2) and $f(x,y)$ are determined uniquely after fixing $Q(x,y)$, according to Eqs. (8). The function ψ_0, defined in this way, certainly satisfies (7). The two vectors in (12), i.e., $(\mu Qa_1,\mu Qa_2)$ and $(-\zeta fa_2,\zeta fa_1)$, are called the gradient and circulation of the drift, respectively. On the one-dimensional set $f(x,y)=0$ (denoted hereafter by Γ_1, if it exists), the circulation alters its direction. If the set $Q(x,y)=0$ (denoted by Γ_2) is nonempty and is a closed curve, and if it does not intersect with Γ_1, the Γ_2 must be a limit cycle of the deterministic system (2). Note that in a bounded system an attracting Γ_2 must be a closed curve. Henceforth, we only consider the case that Γ_2 is closed.

It has been shown[16] that if Γ_1 and Γ_2 do not intersect

each other, ψ_0 is identical to ϕ_0; i.e., ψ_0, calculated from (13), represents the stationary probability distribution of (4) in the leading order of ϵ. If the set $Q(x,y)=f(x,y)=0$ is not empty, ψ_0 and ϕ_0 are no longer identical. Apart from the Hamilton-Jacobi equation (7), ϕ_0 should be constrained to one more boundary condition which is not satisfied by ψ_0. This issue has been clarified in Ref. 16. Nevertheless, ψ_0 still preserves some characteristic feature of ψ_0 (see Figs. 1 and 2 in Ref. 16). Being a Lyapunov function of the deterministic system (2), ψ_0 plays a role similar to the potential. Hence, in what follows, we shall call ψ_0 the potential of the system and focus on the structure of ψ_0, whether it is totally identical to ϕ_0 or not.

Representing the field (C_1,C_2) in the form of (12), we find that the singularities of (2) may have two distinct origins. The first comes from

$$a_1(x,y)=a_2(x,y)=0 \quad \text{(class A)} , \tag{14}$$

and the second from

$$Q(x,y)=f(x,y)=0 \quad \text{(class B)} . \tag{15}$$

In the first case, the potential ψ_0 has local minima, maxima, or saddles at the stable, unstable, and saddle points, respectively. However, in the latter case, the potential ψ_0, determined only by the gradient part of the field, does not feel the alternation of the circulation, i.e., does not feel the sign change of $f(x,y)$. It remains to be flat on the entire curve Γ_2. In Ref. 16, it has been shown that around the two above-mentioned classes of saddles, ϕ_0 also has rather different local structures. It has a local saddle at each saddle point of class A, while there is a discontinuity of its first derivative at those of class B (see Sec. IV in Ref. 16). Thus both functions ϕ_0, which are the potential of the FPE (4), and ψ_0, which is a solution of the Hamilton-Jacobi equation (7) and a Lyapunov function of the deterministic equations (2), reflect the distinction of the two classes of singularities in their different structures.

If we let $\zeta=0$ in (12), Eqs. (2) reduce to a purely gradient system. In case of $\mu=0$, the pure circulation yields a quasi-Hamiltonian system. By quasi-Hamiltonian, we mean that the system may be made a Hamiltonian system by multiplying both equations by a common factor. The multiplicative factor cannot change the track of the trajectory, but it may alter the direction of the trajectory by changing its sign. It is obvious that class-A singular points are stable, unstable, or saddle points of the pure gradient system ($\zeta=0$), and they are elliptic or hyperbolic points of the corresponding quasi-Hamiltonian system ($\mu=0$). On the contrary, for class-B singular points there is no such correspondence. Actually, the one-dimensional curve Γ_1 (or Γ_2) is structurally unstable when $\mu=0$ (or $\zeta=0$), since a planar differential system with degenerate eigenvalues is structurally unstable.[1] Without the circulation (or the gradient), no one-dimensional null set Γ_2 (or Γ_1) can be properly defined at all. Thus class-B singular points may appear only at the presence of both the gradient and circulation.

In order to make Γ_2 (or Γ_1) structurally stable, nonzero circulation (or nonzero gradient) is absolutely necessary. In Ref. 25, one of us has proven that if the circulation does not vanish on Γ_2, the one-dimensional curve Γ_2, i.e., $Q(x,y)=0$, may persist after adding a small perturbation. The same procedure can be applied to prove the structural stability of Γ_1 at the presence of nonzero gradient. Moreover, it can be shown that a small perturbation may only slightly change the functions $Q(x,y)$, $f(x,y)$, $a_1(x,y)$, and $a_2(x,y)$ while retaining the form of (12). Therefore, the form of (12) as well as the classification of the two classes of singular points may be structurally stable.

To conclude this section we present two simplest models to exemplify the singularities of classes A and B.

Model 1:

$$\begin{aligned} \dot{x} &= \mu(ax-x^3)-\zeta(ay-y^3) , \\ \dot{y} &= \mu(ay-y^3)+\zeta(ax-x^3) . \end{aligned} \tag{16}$$

Model 2:

$$\begin{aligned} \dot{x} &= \mu x(a-x^2-y^2)-\zeta y(x^2-y^2-b^2) , \\ \dot{y} &= \mu y(a-x^2-y^2)+\zeta x(x^2-y^2-b^2) . \end{aligned} \tag{17}$$

For model 1, we have

$$\begin{aligned} &Q(x,y)=1, \quad f(x,y)=1 , \\ &a_1(x,y)=ax-x^3, \quad a_2(x,y)=ay-y^3 , \end{aligned} \tag{18}$$

and for model 2,

$$\begin{aligned} &Q(x,y)=a-(x^2+y^2), \quad f(x,y)=(x^2-y^2-b^2) , \\ &a_1(x,y)=x, \quad a_2(x,y)=y . \end{aligned} \tag{19}$$

The potentials are given by

$$\psi_0(x,y)\equiv -\tfrac{1}{4}[2a(x^2+y^2)-(x^4+y^4)] , \tag{20}$$

and

$$\psi_0(x,y)=-\tfrac{1}{4}[2a(x^2+y^2)-(x^2+y^2)^2] , \tag{21}$$

respectively. In case of $a>0$, model 1 has an unstable point (0,0), four stable points $(\pm\sqrt{a},\pm\sqrt{a})$, four saddles $(0,\pm\sqrt{a})$ and $(\pm\sqrt{a},0)$, and one unstable point at infinity. It is obvious that all the singular points belong to class A. The potential ψ_0 takes minina, maxima, and saddles at the stable, unstable, and saddle points, respectively. When $0<a<b^2$, model 2 has a stable limit cycle with an unstable point (0,0) inside it. As $a>b^2$, the closed curve Γ_2, i.e., $a=x^2+y^2$, intersects Γ_1, i.e., $x^2=y^2+b^2$, at four singular points $(\pm[(a+b^2/2)]^{1/2}, \pm[(a-b^2/2)]^{1/2})$, of which two are stable points and the other two are saddles. Apart from the origin, all the singular points apparently belong to class B.

Potentials satisfying (10) have been often used to explore the local and global stability of system (2). However, little has been known beyond that. The relationship between the structure of the potential and the detailed characteristic feature of the dynamics of the deterministic systems has rarely been considered. In the following sections, we shall investigate this aspect in detail. The

function ψ_0, being the Lyapunov function of the deterministic system, must be intrisically related to the dynamic behavior of the system. Since the structure of ψ_0 around singular points of class A are essentially different from that of class B, we expect that the classification into two kinds of singularities should have significant consequence on the deterministic planar system, and these two kinds of singularities should be distinguished not only from the FPE (4), or, equivalently, from the Hamilton-Jacobi equation (7), but also directly from the determimistic flow (2).

III. DETERMINISTIC TRAJECTORY AROUND TWO CLASSES OF SINGULARITIES

Usually, it is difficult to decompose an arbitrary field (C_1, C_2) into the form of (12). Thus a problem of practical importance is whether one can distinguish class-A singular points from those of class B without resort to the explicit form (12). In this paper, we are not yet able to provide a precise criterion. However, from (12) we can already extract some essential features, characteristic for each kind of singularities, by which one may recognize them in certain systems, which cannot be brought into the form (12) analytically.

The following features are worth remarking. Among them the first two stem directly from geometric consideration and the last two from the dynamics.

(1) For class-B singularities, which come from the intersections of two curves, saddle and node must, generically speaking, appear in pairs. Whenever a singular point of class B appears alone, it must be a saddle-node point. Moreover, there must be closed trajectories, connecting the asympototic pairs of singular points of class B. Thus all the singular points that do not satisfy the above constraints must belong to class A. For instance, all the singular points of a bounded system, which cannot be connected by closed trajectories, must be of class A. However, the converse may not be true. Singular points, connected by closed manifolds, can belong to class A as well as to class B [it so happens in both Eqs. (16) and (17)].

(2) The closed curve Γ_2 (assumed to be smooth) must be an invariant manifold of Eqs. (2), and thus no trajectory can cross it. Consequently, no focus can exist on Γ_2. All focuses must belong to class A.

(3) The trajectory of "saddle connection," which is essential for studying the erratic behavior of a forced planar system,[5] can only appear among class-A saddles, while they can never encounter among points of class B. The reason is clear: According to (2) and (12), no pair of saddles of class B can be connected by a single trajectory (heteroclinic orbit) and no saddle of class B can be self-connected by a single trajectory (homoclinic orbit). Nevertheless, both class-A and -B singular points can be connected by homoclinic or heteroclinic trajectories at certain particular parameters. For instance, in (16) heteroclinic orbits exist at $\mu=0$, $a>0$, while in (17) it appears at $a=b^2>0$. However, heteroclinic trajectories, which appear in these two cases, have rather different nature. In the former case, they belong to saddle connection. The saddles are structurally stable against small perturbations. In the latter case, they are saddle-node connections. The saddle-node points can be annihilated by an infinitesimal perturbation.

(4) The bifurcation to a limit cycle in both cases is radically different. In the case of class A, an attracting limit cycle can arise via Hopf bifurcation at which a stable focus is destabilized. According to (2), Hopf bifurcation can never appear for class-B singular points. However, a limit cycle can occur via saddle-node bifurcation among the class-B singular points. For instance, in Eqs. (17), when we decrease a from $a>b^2$ to $a<b^2$, a limit cycle appears beyond the critical point $a=b^2$, at which a saddle-node bifurcation takes place. It is obvious that limit cycles, associated with singular points of class A, can never appear via saddle-node bifurcation. We would like to emphasize that the possibility for a limit cycle to arise via saddle-node bifurcation has been seldom discussed before. However, it should be regarded as one of generic ways for appearance of limit cycles according to Eqs. (12).

From Eqs. (12), we have clear definitions about class-A and -B singularities. However, apart from rather artificial examples such as Eqs. (16) and (17), it is difficult to cast Eqs. (2) into the form of (12) analytically. Moreover, we should admit that our remarks (1)–(4) do not provide a precise criterion to distinguish the two kinds of singular points if the form of (12) cannot be written down explicitly. Nevertheless, these arguments are of importance. On the one hand, they indicate that the classification of two classes of singularities really has some practically observable consequences no matter whether the concrete form (12) can be found or not. On the other hand, they open up the possibility of recognizing the class of singular points in some physically important planar systems as will be shown in Sec. V.

IV. BIFURCATIONS IN PERIODICALLY FORCED PLANAR SYSTEMS

To further investigate the influence of the potential on the dynamics of planar systems, we impose a periodic force on the systems with different kinds of singularities and then study the responses of the systems. This and the next sections will present some numerical results about the bifurcation diagrams in various forced planar systems. With a time-dependent force included, Eqs. (16) and (17) are replaced by

$$\begin{aligned} \dot{x} &= \mu(ax - x^3) - \zeta(ay - y^3) , \\ \dot{y} &= \mu(ay - y^3) + \zeta(ax - x^3) + E\cos(\omega t) , \end{aligned} \tag{22}$$

and

$$\begin{aligned} \dot{x} &= \mu x(a - x^2 - y^2) - \zeta y(x^2 - y^2 - b)/(x^2 + y^2 + 6) , \\ \dot{y} &= \mu y(a - x^2 - y^2) + \zeta x(x^2 - y^2 - b)/(x^2 + y^2 + 6) \\ &\quad + E\cos(\omega t) , \end{aligned} \tag{23}$$

where we put the factor x^2+y^2+6 in the denominator of the circulation only to constrain the trajectory to a limited area in the phase space. To compare with both equa-

tions, we also simulate a periodically forced limit cycle system:

$$\dot{x}=\mu x(a-x^2-y^2)-\zeta y\ ,$$
$$\dot{y}=\mu y(a-x^2-y^2)+\zeta x+E\cos(\omega t)\ , \tag{24}$$

of which the unforced system has the same potential as Eqs. (17). It will soon be shown that the fact that the unforced systems (23) and (24) have the same potential leads to similar characteristic features of the bifurcation structure in the forced systems, though they seem to be rather different in the autonomous case (the former has fixed points as $a>b^2$, while the latter has a single limit cycle). Rather complicated and interesting bifurcation behaviors, such as multiple attractors, transition of basin boundaries from smooth to fractals, hysteresis caused by discontinuous jumps between various attractors, crises, symmetry breaking, and various roads to chaos, can be identified in these models. However, our main interest consists in understanding the influence of the structure of the potential on the dynamics of the forced systems. Therefore, we do not intend to go too far into the details of the bifurcations in the present paper. We only compare the different forced systems by recording the sequences of the bifurcation to subharmonics, quasiperiodicity, and chaos. Even in this aspect, we restrict ourselves on the global bifurcation structure rather than exploring the detail of the bifurcation sequences by invoking much finer resolution. A thorough study of the bifurcation diagram including more aspects and possessing finer resolution will be left for our future work. In all the following calculations, we start from a certain fixed initial condition and vary the amplitude of the force from below, skipping the discussion on the structure of multiple attractors and their basins.

A. Bifurcation diagram of Eq. (22)

Let us first investigate Eqs. (22). Figure 1 schematically plots the bifurcation diagram of Eqs. (22) in ζ-E parameter space. We fix $\mu=a=1$ and vary ζ and E. As B is small, the trajectory moves around the stable point of the unforced system, and the period of the output is identical to that of the force. This kind of trajectory will be called a $1P$ trajectory. The orbit will be called nP subharmonics if the period is n times of that of the driving force. With E increasing, $1P$ motion persists with a larger and larger loop, until the loop reaches the adjacent saddle point. As E is large enough, the trajectory may pass a saddle, getting out of the initial basin and start to travel between various basins (here, by basin, we mean the basin of the unforced system), and the dynamics undergoes dramatic changes. For very large E, the motion is again $1P$. At intermediate values of E, the competition between the external force and the circulation of the system leads to very rich bifurcation patterns. All the parameter regions where the motion is not $1P$ will be called bifurcation regions. Numbers in the figure denote various subharmonics. In the dotted regions, the motion is chaotic or of very long period. It is clear that many periodic windows should be observed by using finer resolution. This remark applies to all figures that follow.

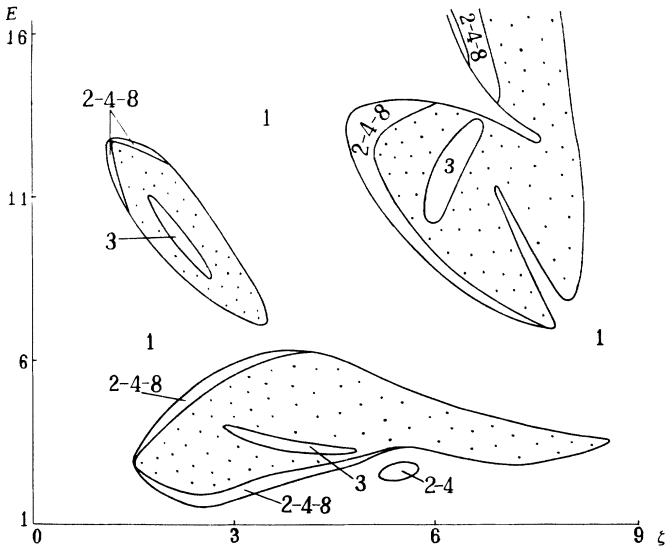

FIG. 1. Bifurcation figure of Eqs. (22). $\mu=a=1$, and $\omega=2\pi$. The numbers in the blank parts of the figure indicate periods of the subharmonics. The dotted region is dominated by chaotic motion. Smaller periodic windows can be found in the chaotic region by finer resolution of detection.

The features of the bifurcation can be summerized as follows.

(1) The prevailing bifurcation sequences are period doublings-chaos-periodic windows-chaos and so on. The largest period window is $3P$ window. The sequence is similar to the U sequence.[26,27] However, the U sequences are often not complete. They are easily interrupted by tangent bifurcations. As ζ is large enough, $1P$ motion can be directly followed by chaos via tangent bifurcation without any subharmonics of higher periods in between. This kind of bifurcation can be identified with type-3 intermittency.[28,29] The various islands of the bifurcation regions can be understood by the basin structure of the potential. When the trajectory alters its basin traveling (i.e., enters a new basin or retreats from an old one by passing a saddle), then bifurcation from $1P$ may take place.

(2) An essential point is that we have never found any information to imply the Farey frequency-locking sequence.[30]

(3) Aperiodic motion is further detected by calculating the Lyapunov exponent. It is found that the largest Lyapunov exponent of the system is always positive whenever the aperiodic motion takes place. We did not find quasiperiodic motion, apart from the accumulating points of certain period-doubling sequences which have zero measure in the parameter space. This finding coincides with the observation that no Farey sequence exists in this system.

B. Bifurcation diagram of Eqs. (24)

Now we are dealing with a typical forced limit cycle system as $a>0$. Figure 2(a) gives the phase figure of the

bifurcations by fixing $a=11$. The blank, shaded, and dotted regions are the periodic, quasiperiodic, and chaotic regions, respectively. There appears a really wide sea of quasiperiodicity. Most of the parameter space is covered by either a quasiperiodic region or the $1P$ region. In the quasiperiodicity sea, one can surely observe Farey frequency-locking sequences as E is small (for instance, $E<22$). Only in the small parts, right on the top of the bifurcation region, can one find period-doubling bifurcation and chaos [which are indicated by I and II in Fig. 2(a)]. This situation radically differs from that in Fig. 1 where period doubling and chaos are prevalent after the system is bifurcated from $1P$. Figure 2(b) is the blowup of region I in Fig. 2(a). Note that we only list the sequence of subharmonics observed by rather rough resolution. Many periods in the quasiperiodic and chaotic regions are not shown. The bifurcation diagram in Fig. 2(a) is essentially identical to that of the sin-circle map[31,32] or, more precisely, to that of the return map recently introduced and investigated in detail by Ding.[33,34]

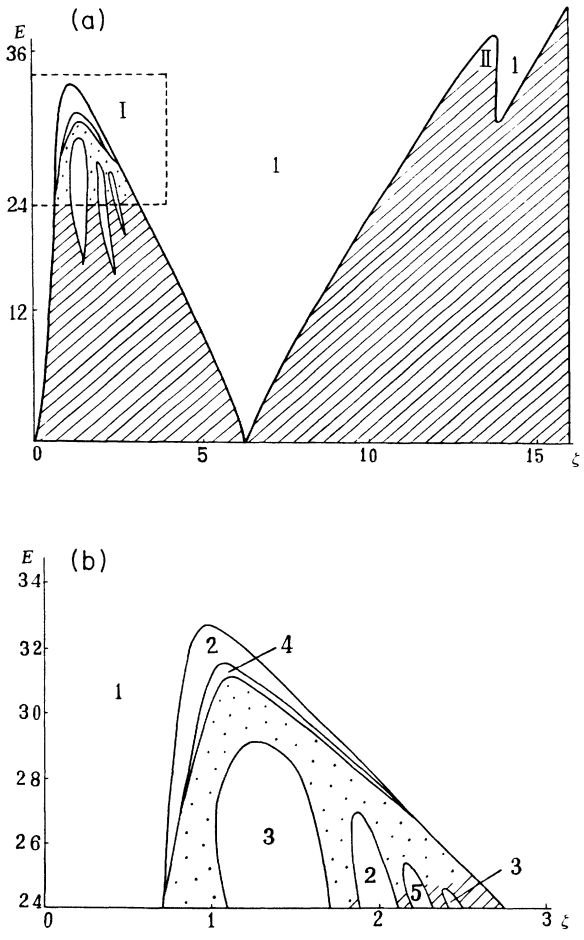

FIG. 2. (a) Bifurcation figure of Eqs. (24). $a=11$, and $\omega=2\pi$. The shaded region denotes quasiperiodicity. Chaos and period-doubling bifurcations can be found in regions I and II, the tops of the bifurcation regions. (b) Enlargement of region I in (a).

C. Bifurcation diagram of Eqs. (23)

For Eqs. (23), we only investigate the case $a>b^2$, when no limit cycle exists in the unforced system. Equations (17) have two saddles and two stable points on the circle $x^2+y^2=a$, which belong to class B. In Fig. 3, we fix $a=9$, $b^2=8$, and have E and ζ varied. The bifurcation figure has the following features.

(1) As E is small and the system is trapped in one of the two attracting basins, the motion is $1P$ that is similar to Eqs. (22). It is stressed that for Eqs. (23), we have *never* found any bifurcation from $1P$ as the system moves only in a single basin.

(2) As E is relatively large, i.e., enough to drive the system out of the initial basin, the bifurcation sequences appear to be completely different from those in Fig. 1. Various subharmonic regions stand one after another very closely, leaving little rooms to quasiperiodicity. Increasing E, the regions of quasiperiodicity becomes a bit wider. The subharmonic periods are apparently of Farey frequency-locking sequence.

(3) Period-doubling bifurcations and chaos can be observed as E is raised to the top of the bifurcation region.

These results are really striking. Both Eqs. (22) and (23) have similar multiple attracting fixed points in the unforced cases, and they are driven by a same force. The responses of both systems are radically different. Neither Farey sequence nor quasiperiodicity have been observed in the system (22) while they are prevailing in (23). The only similar behavior is that the motions are, most probably, $1P$ in both cases as the systems are trapped in a single basin. On the other hand, comparing Eqs. (23) and (24), it seems that they are rather different in the unforced case. The latter contains a single attractor, the limit cycle, while the former has only stable fixed points. However, apart from point (1), the main features of the

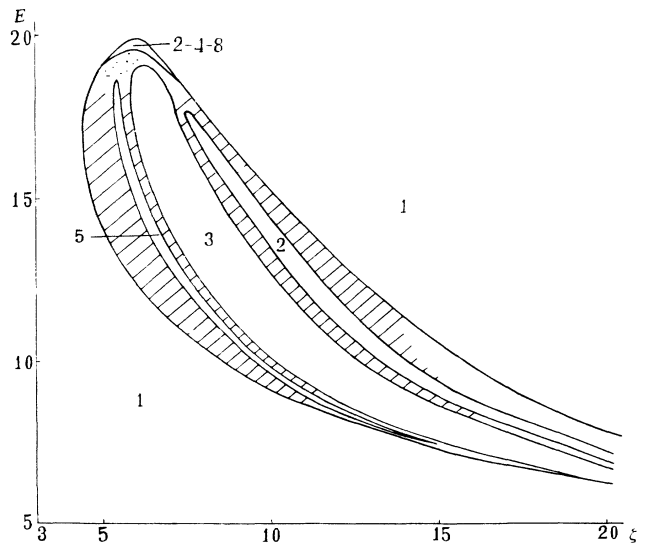

FIG. 3. Bifurcation figure of Eqs. (23). $a=9$, $b^2=8$, and $\omega=2\pi$. The resemblance of this figure with Fig. 2(b) is obvious if we see the part $E>14$ only.

bifurcation structure of (23), i.e., points (2) and (3), are resemblance of those of (24). In both cases, in the lower parts of the bifurcation regions one finds Farey sequences and quasiperiodic motions. Period-doubling bifurcations and chaos may appear for large E, i.e., appear on the tops of the bifurcation regions. In the unforced systems of (23) and (24), the only common feature is that both systems have the same potential. The deviation of the bifurcation schemes of (22) and (23) and the resemblance of those of (23) and (24) strongly suggest that the potential defined by (7) and (13) really has significant and practical consequences, and the systems containing different kinds of singularities may indeed have distinctive dynamic behaviors.

V. DUFFING EQUATION AND THE COUPLED TWO-BOX SCHLÖGL MODEL

Equations (16) and (17) are very typical models for explicitly giving the potential and clearly manifesting the two classes of singular points. It is interesting to study their characteristic features from various aspects. However, in most practical planar differential systems, one cannot specify the potential analytically. Thus, to study some systems, which are of physical interest and do not admit the explicit potentials, is very useful for extending the concept of the potential to more general cases. In this section, we come to examples of this kind. The first model is the well-known Duffing equation

$$\begin{aligned} \dot{x} &= y \ , \\ \dot{y} &= -By + x - x^3 + E\cos(t) \ . \end{aligned} \tag{25}$$

The second example is a coupled two-box Schlögl model. By a suitable transformation, the chemical system of the Schlögl model can be written as[35]

$$\dot{x} = ax - x^3 \ . \tag{26}$$

Let us consider chemical reactions in two boxes of which in each box the uniform concentration of a chemical component follows the reaction-rate equation of the Schlögl model while there is a linear coupling between the two boxes, namely,

$$\begin{aligned} \dot{x} &= ax - x^3 + \zeta y \ , \\ \dot{y} &= ay - y^3 - \zeta x \ . \end{aligned} \tag{27}$$

Moreover, we can input a periodic signal to see the response of the initial autonomous system:

$$\begin{aligned} \dot{x} &= ax - x^3 + \zeta y \ , \\ \dot{y} &= ay - y^3 - \zeta x + E\cos(\omega t) \ . \end{aligned} \tag{28}$$

A. Unforced systems

Let us first analyze both systems without external forces. It is apparent that none of them can be written in the form of (12). Thus no explicit potential is available. However, a remarkable point is that the characteristic features of the potentials in both equations can be qualitatively described. All the singular points of Eqs. (25) belong to class A, while those of Eqs. (27), apart from the origin, belong to class B. These conclusions can be easily justified by the arguments in Sec. III. The reason for the former is simple. There are only three singular points, none of which is saddle-node point. According to the argument (1) in Sec. III, all these singular points can only be of class A. Now we need a bit detailed calculation to justify the conclusion for the latter.

Given $a > 0$, Eqs. (27) contain four stable points and four saddles, which are located, as $\zeta = 0$, at $(\pm\sqrt{a}, \pm\sqrt{a})$ and $(0, \pm\sqrt{a})$, $(\pm\sqrt{a}, 0)$, respectively. Each pair of stable point and saddle move toward each other as indicated in Fig. 4. It is interesting to ask at which a and ζ the stable points lose their stability and by which manner they are destabilized. We may linearize Eqs. (27) at a fixed point (x_s, y_s). The eigenvalue equation reads

$$\lambda^2 - \sigma\lambda + \Omega = 0 \ , \tag{29}$$

with

$$\begin{aligned} \sigma &= 3(x_s^2 + y_s^2) - 2a \ , \\ \Omega &= (3x_s^2 - a)(3y_s^2 - a) + \zeta^2 \ . \end{aligned} \tag{30}$$

The fixed point can change its stability only via crossing two possible critical surfaces: (1) $\sigma = 0$ and (2) $\Omega = 0$.

The first case is impossible since it is easily verified that the system must asymptotically approach the trapping zone

$$0 < a \le x^2 + y^2 \le 2a \ , \tag{31}$$

and then σ must be positive. Thus it is interesting to remark that Hopf bifurcation, which is typical for a limit cycle to appear from a class-A singular point, can never occur in our system. The second case can happen as ζ passes the value

$$\zeta_c^2 = -(3x_c^2 - a)(3y_c^2 - a) \ . \tag{32}$$

At ζ_c, the stable node may lose its stability via saddle-node bifurcation. From Eqs. (27) and (32), x_c, y_c, and ν_c

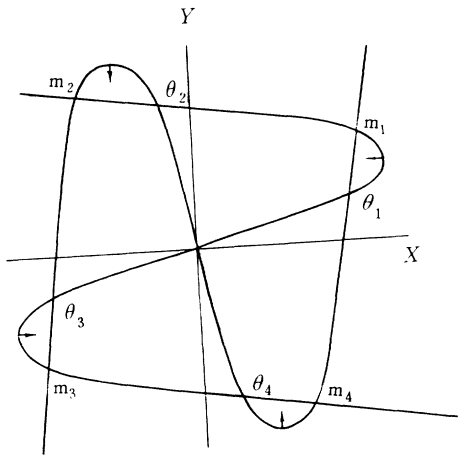

FIG. 4. Curves $y = -(ax - x^3)/\nu$ and $x = (ay - y^3)/\nu$, and the nine fixed points, unstable point (0,0) four stable points m_i, and four saddles θ_i $i = 1, 2, 3$, and 4.

can be solved explicitly in terms of a as

$$x_c=\pm\frac{(3+\sqrt{3}a)^{1/2}}{2},\quad y_c=\pm\frac{(3-\sqrt{3}a)^{1/2}}{2},$$
$$\zeta_c=\frac{a}{\sqrt{8}}. \tag{33}$$

In the parameter region $\zeta>\zeta_c$, there is no fixed point (either stable or unstable) other than the origin, which remains unstable. However, the system is still trapped in the region $a\le x^2+y^2\le 2a$. The only attractor of the system must be a limit cycle. Thus the limit cycle appears exactly via saddle-node bifurcation in the coupled two-box Schlögl model. At the precise value $\zeta=\zeta_c$, heteroclinic trajectories arise at the saddle-node bifurcation point. According to arguments (3) and (4) of Sec. III, the singular points (apart from the origin) must be of class B as ζ is slightly smaller than ζ_c. Moreover, they are expected to belong to the same class for even smaller ζ since the classification of two classes of singularities is structurally stable, and it seems that there is no clear track implying new bifurcation in that region.

B. Bifurcation diagram of Duffing equation

From the discussion in the last subsection, one expects that with a periodic force, Eqs. (25) and (28) should behave in the manner essentially similar to those of Eqs. (22) and (23), respectively. We get the expected results in the numerical simulations of both equations. A great number of publications analyzed the Duffing equation from various aspects.[2,4–7,36–39] However, it is surprising that after an enormous amount of literature, a plot of the bifurcation figure of the Duffing equation in B-E plain, which is important for analyzing the influence of the dissipation on the bifurcation of the forced system, seems to be lacking. Here, in Fig. 5, we attempt to fill this small gap, on the one hand, and to compare with the previous equations (that is our main task), on the other hand.

In Fig. 5, we again avoid the detailed discussion about the multiple attractors and examine the system, starting from small E and fixing the initial condition at $(x_0,y_0)=(2,2)$. All the meanings of the notations in Fig. 5 are the same as those in Fig. 1. Of course, there are bifurcation regions other than that shown in Fig. 5. However, here we only consider the bifurcation region first encountered by increasing E from zero. When E is small and the trajectory is trapped in a single basin, the motion is, in most cases, $1P$. As B is large, period-doubling bifurcations may occur when system is still trapped in a single basin. However, as we observed in Fig. 1, the trajectory certainly reaches the vicinity of the saddle whenever the bifurcation from $1P$ arises. As E is large, the motion turns to $1P$ again. At the intermediate values of E, the trajectory travels in the double basins and gives an interesting bifurcation-phase portrait.

Usually, chaos appears as soon as the trajectory starts to wander in the double basins. There appear various period windows in the chaos sea. Period-doubling bifurcation sequences can be found around the border of the bifurcation region as well as in the period windows. We cannot find quasiperiodic motion except at the accumulation points right before chaos bursts which have, actually, zero measure in the parameter space just like what happens in Fig. 1. When the motion is aperiodic, the largest Lyapunov exponent is surely positive. By a careful detection, we did not find a Farey frequency-locking sequence. The prevailing bifurcation are period-doubling bifurcations, leading to chaos and period windows in the chaos regions. Again, the bifurcation sequence is often abruptly interrupted by tangent bifurcation halfway. These futures can be well understood by the cubic map which is suggested by Holmes to represent the Poincaré map of the Duffing equation.[5,36] The numerical results show that the Duffing equation has a bifurcation structure similar to Eqs. (22). It is consistent with the fact that both of them have a similar potential (i.e., they have the same class-A singular points) in the unforced cases.

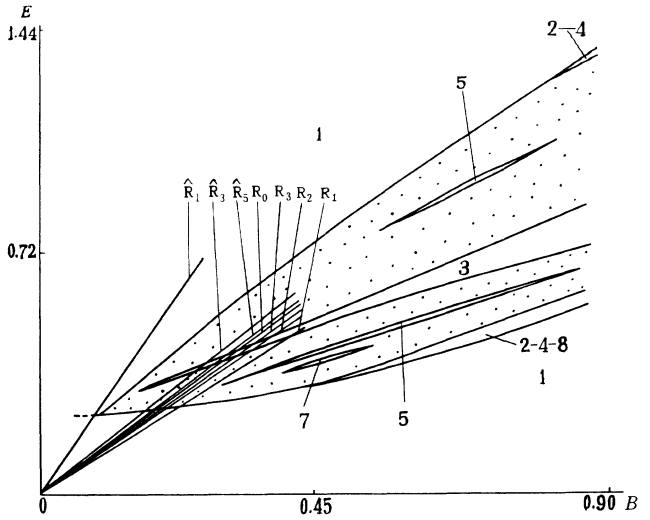

FIG. 5. Bifurcation figure of the Duffing equation (25). Period-doubling bifurcation and chaos are prevalent in the bifurcation region. No Farey sequence is observed. All R_n, $\hat{\mathbf{R}}_n$, and R_0 are plotted according to the theoretical results of the Melnikov method. R_n indicates the critical condition for n subharmonics of which the trajectory is trapped in a single potential well, while $\hat{\mathbf{R}}_n$ indicates the circles around a large loop including both wells. R_0 denotes the threshold for the transverse crossing of the stable and unstable manifolds of the saddle. No visible agreement between the theoretical plots and numerical results exists.

Up to date, the only analytical and relatively general way in dealing with the bifurcation to subharmonics and chaos in the forced planar differential system is the Melnikov method. It is considered to be valid, as the external force and the dissipation are weak and the autonomous system is near the parameters of the orbit of certain periods or that of homoclinic (or heteroclinic) orbit. Recently, some numerical results indicated that the Melnikov function is not a good criterion for predicting chaotic attractor. Its threshold is often lower, sometimes much lower, than the true boundary of observable chaotic motion.[38,40] It is suggested[38,40] that the transverse intersection of stable and unstable manifolds predicted by the Melnikov function might have some rela-

tion with the fractal structure of the basin boundary. With the arguments in Sec. III and the phase portrait of Fig. 5, we would like to make some further remarks on the Melnikov method.

First, it is obvious that the Melnikov function criterion for the transverse crossing of stable and unstable manifolds of the homoclinic (or heteroclinic) orbit cannot be applied to the orbit connecting class-B singular points, for instance, to Eqs. (23) and (28) (as $a=b^2$ and $\zeta=\zeta_c$, there indeed exist heteroclinic orbits). The heteroclinic orbits connecting class-B singular points are not the saddle connected orbit. In fact, a small perturbation may definitely destroy the saddle-node points, and then no more stable and unstable manifolds of the unforced system remain at all. This fact is substantially different from the situation of class-A points where the saddle points are structurally stable against small perturbations. Second, even for Eqs. (22) and the Duffing equation (25), which serves as the most typical example for the application of the Melnikov method, the Melnikov function poorly predicts observable chaotic motion and subharmonics. In Fig. 5, the various straight lines predicted by the Melnikov function for subharmonics and chaos[2] are presented to compare with the numerical results. R_n indicates the critical condition for n subharmonics of which the trajectory is trapped in a single potential well, while $\hat{R}_n$ indicates that of the trajectory circling around large loops including both wells. R_0 denotes the threshold for the transverse crossing of the stable and unstable manifolds of the saddle. For chaotic motion, our result agrees with Refs. 38 and 40 where for small B the Melnikov criterion is lower than the actual threshold of chaos. What we would like to emphsize here is that for the criterions of subharmonics, the correspondence is even poorer. Actually, there is not a visible correspondence between the theoretical predictions and numerical results. According to the theoretical analysis, various periodic orbits should appear before and after R_0. These orbits may possibly appear as the ratios of the periods of the unperturbed orbits to the period of the force are rational numbers. It suggests a certain kind of period-adding sequence (see the straight lines of Fig. 5 and those in Fig. 4.6.3 in Ref. 2) and, possibly, quasiperiodicity in between. However, so far no such kinds of bifurcation sequence and quasiperiodicity have been observed. When the system is trapped in a single basin, we find $1P$ in most cases or period-doubling leading to chaos in a narrow parameter region in which the trajectory passes by in close vicinity to the saddle. No sequence of subharmonics indicated by R_n, $n=2m+1$, $m=0,1,2,\ldots$, has been found. When the trajectory flies among the different basins, one again finds period doubling and, in most cases, chaos and narrow period windows. The straight lines predicted by the Melnikov function have nothing to do with the actual bifurcation boundaries in any cases of Fig. 5. The most serious problem is the complete inconsistence of the theoretical and numerical results at small dissipation and forcing. It is expected that the Melnikov method, based on the perturbation procedure, must work better for small B and E. However, the results are to the contrary. As B and E are small, no subharmonics or chaos exists. It seems that a small perturbation may offer a radical change of the bifurcation figure to Hamiltonian systems since, as $B=0$, the motion of the forced system of (25) is very much deviated from that of $0<B\ll 1$, where the response of the unforced system to the periodic force is purely $1P$ whatever E in Fig. 5. This observation is sharply in contradiction with the Melnikov theory.[2,41] This disagreement in the Duffing equation should be carefully examed since the Duffing equation has been so extensively used to demonstrate the Melnikov method.

C. Bifurcation diagram of the forced two-box Schlögl model

As expected, the bifurcation phase portrait of Eqs. (28) differs radically from that of the Duffing equation, while it is essentially identical to that of Eqs. (23). In Fig. 6, we fix $\zeta=8$ and vary E, and $a>a_c=\sqrt{8\zeta}$. Thus no limit cycle exists for the given parameters. When E is small and the system is trapped in a single region, we *always* find $1P$ motion. For very large B, the system can be completely controlled by the force and has $1P$ motion again. At the intermediate values of E, the force is large enough to drive the system travel in various basins and is still not strong enough to completely control the system; then one may find bifurcation regions where various bifurcations to subharmonics, quasiperiodicity, and chaos arise. In the bifurcation region at relatively small E, one finds an apparent Farey frequency-locking sequence and quasiperiodicity between the various period regions. Period-doubling bifurcations and chaos can only be observed in a small region of large E; actually, they can be found only on the top of the bifurcation region. These features are the same as those of Eqs. (23). The head of the bifurcation region is not shown in Fig. 6 because one cannot see the extension. (One cannot see the head after $E>300$.) The bifurcation structures of both Eq. (23) and (28) are similar to that of the forced limit cycle system (24) although they have no limit cycle at all without the external force. The only common feature of all these three unforced systems is that they have the similar potentials of

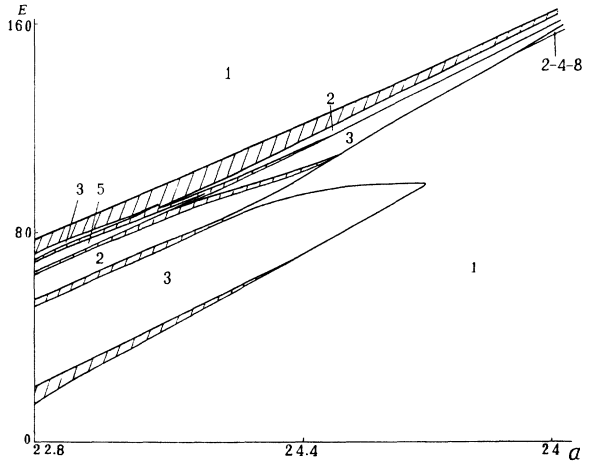

FIG. 6. Bifurcation figure of Eqs. (28). $\zeta=8$, and $\omega=2\pi$. All the notations are the same as in Fig. 2.

which each takes a minimal value at a one-dimensional set Γ_2.

All the findings in the present section are favorable for the following two conclusions. On the one hand, the structure of the potential defined in Sec. II or, say the classification of the two kinds of singularities based on the potential forms (12) and (13) really have physical consequence. On the other hand, the arguments in Sec. III may be successfully used for clarifying the potential and distinguish the classes of the singularities when the form Eqs. (12) cannot be obtained explicitly. The second conclusion is very much desirable for applying the analysis of this paper to more general and physically relevant situations.

VI. CIRCULATION, POTENTIAL, AND BIFURCATIONS

By dividing the drift of the FPE (4) or, say, the field of the differential equations (2) into a gradient part and a circulation, we defined the potential of the system, ψ_0, which is a Lyapunov function of the deterministic system and is related to the stationary solution of the FPE in the sense stated in Sec. III. Then we classified two kinds of singularities around which the potential has substantially different structures and revealed how the dynamics of the autonomous planar systems and the corresponding forced planar systems is affected by the different potential structures in the vicinities of these two classes of singular points. In this section, we summarize the main findings in all our models.

A remarkable point is that the existence of the circulation seems to be necessary for the forced systems to bifurcate from $1P$ motion. If an autonomous planar system is purely gradient [i.e., $f(x,y)\equiv 0$ in Eqs. (12)], one can never find any attracting trajectory other than $1P$ orbit when the system is forced by a periodic input. We have examined this fact by taking various equations and varied the control parameters in wide regions. For instance, for all Eqs. (22), (23), (24), and (28), one can find nothing but $1P$ motion without the circulations (i.e., put $\zeta\equiv 0$) no matter how we change a, E, and ω. We have replaced $(-\zeta y,\zeta x)$ in Eqs. (28) by $(-\zeta(x-y),\zeta(x-y))$. This slight change in the linear terms completely alters the results. Now the autonomous system,

$$\begin{aligned}\dot{x}&=ax-x^3-\zeta(y-x)\ ,\\ \dot{y}&=ay-y^3-\zeta(x-y)\ ,\end{aligned}\tag{34}$$

becomes a two-box diffusion Schlögl model (see Refs. 42 and 43). The essential change is that now Eqs. (34) become purely gradient and the corresponding FPE (4) satisfies detail balance. Applying a periodic force on (34) and examining the output in a wide region by changing a, ζ, E, and as well as the frequency of the force, only $1P$ motion can be found. We have not yet succeeded in understanding this matter. However, no evidence is against this observation.

All the models considered in the presentation have multiple fixed-point attractors in the autonomous cases apart from Eqs. (24), which has a single limit cycle attractor. In the multiple-basin cases, the bifurcation of the forced system from $1P$ motion can be observed only as the trajectory reaches the vicinity of a saddle point or passes over saddle points to circle about various static equibria of the autonomous system. With class-B stable points, bifurcation from $1P$ has never been found in our simulation when the system is trapped in a single basin. For class-A singular points, period doubling leading to chaos may be found before (but very near) the trajectory passes the saddle and enters new basins.

Note that all the above is observed in multibasin systems. By attracting basins, we mean the potential basins which are identified without the external force. However, only the attracting basins of the weakly forcing system can be approximately characterized by those of the autonomous system. Then the previous argument makes sense only if the forcing is not too strong. When E is very large, the trajectory takes large loops and does not feel the multiple basins of the unforced system at all. Thus all bounded systems can be regarded as a one-potential-well system for very large E. There have been many publications considering one-potential-well systems, such as the forced soft spring system,[44] the Duffing equation with positive stiffness,[34,45] the Duffing equation with unbounded trajectory,[46] and so on. It has been shown that a strong force may completely change the basin structure of the unforced system. We believe that a comparison of forced one-potential-well planar systems with those of multiple-potential-well systems will be useful for understanding the bifurcation mechanisms in different potentials.

When a planar system is driven by a periodic force to the bifurcation conditions, two kinds of responses are observed as we have stated in Secs. IV and V. A striking point is that these two kinds of behavior do exist in many systems. Actually, most of the known forced planar systems of physical importance can be brought into one of these classes. All forced limit cycle systems, such as the forced Van der Pol oscillator, including its various modifications,[47] and the forced Brusselator,[48–50] may have a similar behavior such as Eqs. (24), (23), and (28) when the trajectory is not too far from the limit cycle of the autonomous system. The other systems, such as the Duffing equation, the Josephson junction system[51–53], the superconduct quantum interference device (SQUID) system,[40] and so on, have a behavior similar to Eqs. (22) and (25). It can be easily examined that for the latter class of equations, all the singular points, around which the trajectory may travel at the parameters taken, are of class A. In this presentation, for the first time, we point out that systems like Eqs. (23) and (28) may behave like a forced limit cycle system, although the autonomous system contains no limit cycle. These systems must have singularities of class B which are considered to generically exist and to be structurally stable. In fact, the two-box coupled Schlögl model is rather typical, and it represents a large class of the systems. For instance, two independent one-dimensional differential equations with multiple basins can fall into the class of (27) when they coupled by linear curl terms. In this presentation, we show two different ways to make a limit cycle of the autonomous

system disappear. One way is via Hopf bifurcation; then the limit cycle turns out to be smaller and smaller, and finally collapses to a fixed point. The other is via saddle-node bifurcation; then the limit cycle turns slower and slower, and finally vanishes at a finite circle via a "crisis." It is interesting to see that, by applying a periodic signal the characteristic features of the limit cycle system are lost after the limit cycle disappears in the former case, while still being kept in the latter case.

More complicated systems may produce more complex bifurcation figures. For instance, more islands of bifurcation regions may exist; the two kinds of bifurcation figures may appear, simultaneously, in a single system in different parameter regions or different variable ranges if such a system contains both kinds of singularities.

VII. POTENTIAL, CLASSIFICATION OF SINGULARITIES, AND GENERAL FOKKER-PLANCK EQUATIONS

Up to now, the study of the structure of the potential and the classification of singularities has been based on the potential originating from the Hamilton-Jacobi equation (7), which was derived from the FPE (4). Different kinds of noises may be added to the deterministic Eqs. (2) and result in rather distinctive FPE's. Now problems of conceptional importance arise: whether the classification of the two classes of singularities makes sense if the noise added to the deterministic equations are different from (3), and whether the classifications of the singularities from different kinds of FPE's are identical. A negative answer to any of the above may substantially limit the significance of all the previous results. It is very much appreciated that the answers are positive.

Let us start from the most general two-dimensional Langevin equations:[14]

$$\begin{aligned}\dot{x}&=C_1(x,y)+\sqrt{\epsilon}[k_{11}\hat{\gamma}_1(t)+k_{12}\hat{\gamma}_2(t)]\ ,\\ \dot{y}&=C_2(x,y)+\sqrt{\epsilon}[k_{21}\hat{\gamma}_1(t)+k_{22}\hat{\gamma}_2(t)]\ ,\end{aligned}\tag{35}$$

with

$$\begin{aligned}&\langle\hat{\gamma}_1(t)\rangle=\langle\hat{\gamma}_2(t)\rangle=\langle\hat{\gamma}_1(t)\hat{\gamma}_2(t')\rangle=0\ ,\\ &\langle\hat{\gamma}_1(t)\hat{\gamma}_1(t')\rangle=2\delta(t-t')\ ,\\ &\langle\hat{\gamma}_2(t)\hat{\gamma}_2(t')\rangle=2\delta(t-t')\ .\end{aligned}$$

Since we are concerned with only the leading terms of ϵ, the Stratonovich or the Ito interpretations on the stochastic processes do not make a difference. In the weak-noise limit, the Langevin equations (35) can be transformed to the FPE:

$$\begin{aligned}\frac{\partial p(x,y,t)}{\partial t}=&-\frac{\partial}{\partial x}[C_1(x,y)p(x,y,t)]\\ &-\frac{\partial}{\partial y}[C_2(x,y)p(x,y,t)]\\ &+\epsilon\left[h_{11}\frac{\partial^2}{\partial x^2}+h_{22}\frac{\partial^2}{\partial y^2}\right.\\ &\left.+2h_{12}\frac{\partial^2}{\partial x\,\partial y}\right]p(x,y,t)\ ,\end{aligned}\tag{36}$$

with

$$\begin{aligned}&h_{11}(x,y)=k_{11}^2+k_{12}^2,\quad h_{22}(x,y)=k_{21}^2+k_{22}^2\ ,\\ &h_{12}(x,y)=2(k_{11}k_{21}+k_{12}k_{22})\ .\end{aligned}\tag{37}$$

It is obvious from (37) that the diffusion matrix of (36) is non-negative for any (x,y). Inserting

$$\begin{aligned}p(x,y)=N\exp\left[-\left[\frac{\hat{\phi}_0(x,y)}{\epsilon}+\hat{\phi}_1(x,y)\right.\right.\\ \left.\left.+\epsilon\hat{\phi}_2(x,y)+\cdots\right]\right]\end{aligned}\tag{38}$$

into Eq. (36) and keeping only the leading terms of $1/\epsilon$, we arrive at the general Hamilton-Jacobi equation

$$\begin{aligned}&\left[C_1(x,y)+h_{11}\frac{\partial\hat{\phi}_0}{\partial x}+h_{12}\frac{\partial\hat{\phi}_0}{\partial y}\right]\frac{\partial\hat{\phi}_0}{\partial x}\\ &+\left[C_2(x,y)+h_{12}\frac{\partial\hat{\phi}_0}{\partial x}+h_{22}\frac{\partial\hat{\phi}_0}{\partial y}\right]\frac{\partial\hat{\phi}_0}{\partial y}=0\ .\end{aligned}\tag{39}$$

Suppose that we are able to divide the drift (C_1,C_2) to the following form:

$$\begin{aligned}C_1(x,y)&=h_{11}g_1(x,y)+h_{12}g_2(x,y)+d_1(x,y)\ ,\\ C_2(x,y)&=h_{12}g_1(x,y)+h_{22}g_2(x,y)+d_2(x,y)\ ,\end{aligned}\tag{40}$$

with

$$\begin{aligned}&\frac{\partial g_1}{\partial y}=\frac{\partial g_2}{\partial x}=-\frac{\partial^2\hat{\psi}_0}{\partial x\,\partial y}\ ,\\ &g_1d_1+g_2d_2=0\ .\end{aligned}\tag{41}$$

It is evident that the function $\hat{\psi}_0(x,y)$ must be a solution of the Hamilton-Jacobi equation (39) and a Lyapunov function of the deterministic system (2):

$$\hat{\psi}_0=-(h_{11}g_1^2+h_{22}g_2^2+2h_{12}g_1g_2)\le 0\ ,\tag{42}$$

due to the non-negative of the diffusion matrix. Thus $\hat{\psi}_0$ must take extrema at all the asymptotic sets of (2). Let us consider a limit cycle system. $\hat{\psi}_0$ should take extrema at the entire circle of the limit cycle, namely, the constraints

$$g_1=\frac{\partial\hat{\psi}_0}{\partial x}=g_2=\frac{\partial\hat{\psi}_0}{\partial y}=0\tag{43}$$

must be hold on a one-dimensional closed curve. Thus it is convenient to rewrite (g_1,g_2) by (Qa_1,Qa_2) as we did for (8). Then Eqs. (40) can be replaced by

$$\begin{aligned}C_1(x,y)=&\mu\hat{Q}(x,y)[h_{11}\hat{\mathbf{a}}_1(x,y)+h_{12}\hat{\mathbf{a}}_2(x,y)]\\ &-\nu\hat{\mathbf{f}}(x,y)\hat{\mathbf{a}}_2(x,y)\ ,\\ C_2(x,y)=&\mu\hat{Q}(x,y)[h_{12}\hat{\mathbf{a}}_1(x,y)+h_{22}\hat{\mathbf{a}}_2(x,y)]\\ &+\nu\hat{\mathbf{f}}(x,y)\hat{\mathbf{a}}_1(x,y)\ ,\end{aligned}\tag{44}$$

$$\frac{\partial(\hat{Q}\hat{\mathbf{a}}_1)}{\partial y}=\frac{\partial(\hat{Q}\hat{\mathbf{a}}_2)}{\partial x}=-\frac{\partial^2\hat{\psi}_0}{\partial x\,\partial y}\ .\tag{45}$$

Now the drift can no longer be divided to a pure gradient

part and a vertical circulation as we did for (7). Nevertheless, the functions $\hat{Q}(x,y)$ and $\hat{f}(x,y)$ still have similar meanings as $Q(x,y)$ and $f(x,y)$ in (12). Let us call the sets $\hat{f}=0$ and $\hat{Q}=0$, $\hat{\Gamma}_1$ and $\hat{\Gamma}_2$, respectively. According to (44), we again find that the singularities of Eqs. (2) come from two origins:

$$\begin{aligned} &\hat{a}_1(x,y)=\hat{a}_2(x,y)=0, \quad \text{class A} \\ &\hat{Q}(x,y)=\hat{f}(x,y)=0, \quad \text{class B} . \end{aligned} \tag{46}$$

With class-A singular points, the potentials $\hat{\psi}_0$ really take local minima, maxima, and saddles at the stable, unstable, and saddle points, while with class-B singularities, the potential remains flat on the entire circle $\hat{\Gamma}_2$. The situation is exactly the same as that encountered for (12) in Sec. II.

The problem remaining is to identify the two sets of (46) to those of (14) and (15). The identification is convincing if we notice that all the arguments in Sec. III are completely valid for class-A and -B singular points defined in (46). Now many FPE's, or precisely, many Hamilton-Jacobi equations, which are different owing to distinct noises, correspond to a unique set of deterministic equations (2). For classifying the two classes of singularities, each Hamilton-Jacobi equation requires the same conditions (Sec. III). For instance, for a limit cycle system, all $\hat{\Gamma}_2$ must be identical to the same limit cycle whatever the diffusion matrix of Eq. (36). As the limit cycle disappears via saddle-node bifurcation, the singular points appearing in the deterministic system (2) must be of class B. This fact is not affected by the difference of the noises. In fact, it is easy to prove that the curves $\hat{\Gamma}_2$ defined for different noises must identical no matter whether the limit cycle exists or not (i.e., no matter whether $\hat{\Gamma}_1$ and $\hat{\Gamma}_2$ intersect each other or not).

Actually, as $k_{11}=k_{22}=1$ and $k_{12}=k_{21}=0$, Eqs. (45) and (46) recover (12) and (14), (15), respectively. It is reasonable to conclude that as we slightly change the form of noises, the classes of the singularities of the potential must remain the same while the form of the potential is modified. By continuously varying the noises bit by bit, the conclusion must remain truly independent of the noise form. Then the identity between (14), (15), and (46) is rigorously proved. Thus the classification of the singularities should be considered as the intrinsic property of the deterministic equations (2) since it is independent of the concrete form of the noises.

The above justification may tremendously enlarge the application range of the potential analysis. Given certain deterministic planar equations, an explicit form of Eqs. (46) may not be available for certain noises, but it can be analytically presented for an alternative choice of Langevin forces. Thus the possibility of finding an analytic form of the potential may be considerably enlarged by properly choosing the noises. For instance, with the unforced Duffing equations (25), no explicit solution of (12) can be obtained. However, if the noises are given by $k_{11}=k_{12}=k_{21}=0$ and $k_{22}=1$, Eq. (39) can be exactly solved, namely,

$$\hat{\phi}_0=\hat{\psi}_0=\tfrac{1}{2}ay^2-\tfrac{1}{4}a(2x^2-x^4) . \tag{47}$$

Thus one can definitely conclude that all the singular points in the Duffing equation are of class A because they directly come from the extreme points of the potential. This conclusion justifies our analysis in Sect. V and shows that the discussion based on the arguments of Sec. III is reasonable. In fact, for a large class of deterministic equations

$$\begin{aligned} &\dot{x}=y , \\ &\dot{y}=-ay+f(x) , \end{aligned} \tag{48}$$

which are nonlinear oscillators with linear damping and include all the Duffing equations, the Josephson junction equations, the SQUID system, and so on without forcing its special forms, the classification of the singularities can be identified. With the noninvertible diffusion matrix ($h_{22}=1$, and all the other elements of the diffusion matrix vanish), we may easily identify

$$\hat{\phi}_0=\hat{\psi}_0=\tfrac{1}{2}ay^2-a\int f(x)dx , \tag{49}$$

which is the exact solution of the well-known Kramers equation.[11] Therefore, all the singular points in this kind of equation are of class A. According to our observations in Secs. IV and V, we may conjecture that they should behave as Eqs. (22) and (25) with a periodic forcing.

The finding in this section is significant. $\hat{\phi}_0$, representing the stationary solution of the FPE (36) in the weak-noise limit [see (38)], is identical to $\hat{\psi}_0$ if no intersection of $\hat{\Gamma}_1$ and $\hat{\Gamma}_2$ exists. When the intersections of both curves exist, $\hat{\phi}_0$ differs from $\hat{\psi}_0$. $\hat{\phi}_0$ really has a local saddle at the saddle points of class A, while it has a discontinuity of its first-order derivative at those of class B. (For details, we refer to Ref. 16). Thus for $\hat{\phi}_0$ the two classes of singularities of the deterministic equations (2) are also distinguished. Probability of the FPE is a measurable quantity. By measuring the stationary probability distribution of the FPE with small diffusion strength, one may realize the form of (44) and practically distinguish the two kinds of singular points indeed, no matter whether we can analytically realize (12) and (44) or not. Since the FPE has been extensively used to study the potential of nonequilibrium systems, the results of this work may be a useful step toward a better understanding of the evolution of the macroscopic variables on the basis of their nonequilibrium potential.

VIII. SOME OPEN PROBLEMS

The present paper suggests a classification of two kinds of singular points based on distinct potential structures and emphasizes the influence of the potential on the deterministic systems in both of the autonomous and periodically forced circumstances. Nevertheless, several problems are open. Despite some reasonable analytic arguments and numerical observations that validate the classification, no mathematically precise criterion is defined to distinguish the two kinds of singular points. The transition from one kind of singularities to the other may be regarded as a sort of phase transition, and it can occur only under some critical conditions. It is still open as to how to specify the critical conditions. It is numeri-

cally observed that the outputs of the forced systems are radically different if the singular points the trajectory circles around are different. The mechanisms underlining these observations are still unknown. The models suggested in the presentation deserve further investigation by some other methods, for instance, by examing the features of the trajectory, extracting the corresponding return map, clarifying the symbolic dynamics, detecting the basin boundaries, or manifesting the multifractal structure of the strange attractors and so on. They will be our future works. We hope that the present work may stimulate a study treating forced planar differential equations in various groups, such as one-potential-well systems, multiple-potential-well systems, forced limit cycle systems, systems with class-A or -B fixed-point basins, and so on, and clarifying the common features of bifurcations in each group and main differences in distinct groups.

ACKNOWLEDGMENTS

We thank M. H. Jensen for fruitful discussions.

[1]V. I. Arnold, *Geometrical Method in the Theory of Ordinary Differential Equations* (Springer, New York, 1982).
[2]J. Guckenheimer and P. Holmes, *Nonlinear Oscillations, Dynamical Systems, and Bifurcations of Vector Field* (Springer, New York, 1983).
[3]B. V. Chirikov, Phys. Rep. **52**, 265 (1979).
[4]F. C. Moon and P. J. Holmes, J. Sound Vib. **65**, 275 (1989).
[5]P. J. Holmes, Philos. Trans. R. Soc. A **292**, 419 (1979).
[6]C. Holmes and P. J. Holmes, J. Sound Vib. **78**, 162 (1981).
[7]F. C. Moon and G. Li, Physica D **17**, 99 (1985).
[8]J. Guckenheimer, Physica D **1**, 227 (1980).
[9]R. Graham and H. Haken, Z. Phys. **243**, 289 (1971).
[10]H. Haken, *Advanced Synergetics* (Springer, Berlin, 1984).
[11]H. Risken, *The Fokker-Planck Equation* (Springer, New York, 1983).
[12]R. Graham and A. Schenzle, Z. Phys. B **52**, 61 (1983).
[13]R. Graham and T. Tel, Phys. Rev. A **31**, 1109 (1985).
[14]R. Graham, D. Roekaerts, and T. Tel, Phys. Rev. A **31**, 3364 (1985).
[15]G. Hu, Phys. Rev. A **38**, 3693 (1988).
[16]G. Hu, Phys. Rev. A **39**, 1286 (1989).
[17]G. Hu and H. haken, Phys. Rev. A **40**, 5966 (1989).
[18]G. Hu and H. Haken, Phys. Rev. A **41**, 2231 (1990).
[19]T. Tel, R. Graham, and G. Hu, Phys. Rev. A **40**, 4065 (1989).
[20]R. Benzi, S. Sutera, and A. Vulpiani, J. Phys. A **14**, L453 (1981).
[21]C. Nicolis, Tellus **34**, 1 (1982).
[22]P. Jung and P. Hanggi, Europhys. Lett. **8**, 505 (1989).
[23]R. Fox, Phys. Rev. A **39**, 4148 (1989).
[24]B. McNamara and K. Wiesenfield, Phys. Rev. A **39**, 4854 (1989).
[25]G. Hu, Commun. Theor. Phys. **9**, 35 (1989).
[26]N. Metropolis, M. L. Steinm, and P. R. Stein, J. Combinat. Theory **15**, 25 (1973).
[27]M. J. Feigenbaum, J. Stat. Phys. **19**, 25 (1978).
[28]Y. Pomeau and P. Manneville, Commun. Math. Phys. **77**, 189 (1980).
[29]H. Bunz, H. Ohno, and H. Haken, Z. Phys. B **56**, 345 (1984).
[30]K. Kaneko, Prog. Theor. Phys. **68**, 669 (1982).
[31]J. Bélair and L. Glass, Physica D **16**, 143 (1985).
[32]M. H. Jensen, P. Bak, and T. Bohr, Phys. Rev. Lett. **50**, 1637 (1983).
[33]E. J. Ding, Phys. Rev. A **34**, 3547 (1986).
[34]E. J. Ding, Phys. Rev. A **36**, 1488 (1987).
[35]F. Schlögl, Z. Phys. **245**, 141 (1971).
[36]B. Hu and J. M. Mao, Phys. Rev. A **27**, 1700 (1983).
[37]C. Holmes and P. Holmes,J. Sound Vib. **78**, 161 (1981).
[38]F. C. Moon and G.-X. Li, Phys. Rev. Lett. **55**, 1439 (1985).
[39]C. Pezeshki and E. H. Dowell, Physica D **32**, 194 (1989).
[40]E. W. Jacobs and A. R. Bulsara, Physica D **34**, 439 (1989).
[41]P. Holmes and D. Whitley, Physica D **7**, 111 (1983).
[42]G. Hu, J. Phys. A **21**, 365 (1989).
[43]G. Hu and H. Haken, Z. Phys. B **76**, 537 (1989).
[44]Y. Ueda, Int. J. Nonlinear Mech. **20**, 481 (1985).
[45]T. Fang and E. H. Dowell, Int. J. Nonlinear Mech. **22**, 267 (1987).
[46]Y. H. Kao, J. C. Huang, and Y. S. Gou, Phys. Lett. A **131**, 91 (1988).
[47]S. Rajasekar and M. Lakshmanan, Physica D **32**, 146 (1988).
[48]K. Tomita, Phys. Rep. **86**, 113 (1982).
[49]B.-L. Hao and Zhang S.-Y., J. Stat. Phys. **28**, 769 (1982).
[50]B.-L. Hao, *Elementary Symbolic Dynamics and Chaos in Dissipative Systems* (World Scientific, Singapore, 1989), pp. 287–325.
[51]R. L. Kautz and R. Monaco, J. Appl. Phys. **57**, 875 (1985).
[52]W. J. Yeh and Y. H. Kao, Phys. Rev. Lett. **49**, 1888 (1982).
[53]E. G. Gwinn and R. M. Westervelt, Phys. Rev. A **33**, 4143 (1986).